For γ below γ_c the forearc behaves elastically (i.e., $\psi = \gamma$). For γ greater than γ_c the motion of the forearc (averaged across the forearc) is assumed to be proportional to the trench-parallel component of the plate vector minus the slip vector at $\gamma=\gamma_c$. The parameter α is the ratio of the across-arc average of the forearc's trench-parallel velocity to the trench-parallel velocity of the subducting plate (minus the slip vector at $\gamma=\gamma_c$), both in a reference frame in which the rigid part of the upper plate is fixed. Hence, α varies from 0 (oblique thrusting and no deformation of the upper plate; elastic) to 1 (complete decoupling). For example, a viscous forearc across which the trench-parallel velocity decreases linearly would have α=0.5 and γ_c=0° while an across-arc exponential decrease in velocity would give α=0.7. Using the observed $\psi(\gamma)$ for all of the world's major trenches and a χ^2 test, we can constrain the mechanical behavior of the forearcs by finding the most probable ranges of α and γ_c to match the observations. Candidates for elastic behavior (low α or high γ_c) are Japan, Kuriles, S America, Middle America, Solomon, and Tonga forearcs; at these the slip vectors do not deviate significantly from the plate vectors. Elastic-perfectly plastic behavior (α=1, γ_c>0) is seen at the Antilles, New Britain, New Hebrides, and Ryukyu forearcs. Elastic-plastic behavior (0.4<α<1, γ_c>0) is seen at the Aleutian and Sumatran forearcs while the Izu-Mariana, Philippine, and Sandwich forearcs appear to behave viscously (0.4<α<0.8, γ_c=0).

T32C-4 1415h

The Significance of Lower Crust Rheology at Transpressional Plate Margins

M L Hill (Department of Geology, Temple University, Philadelphia, PA 19122; 215-787-8226)

Oblique convergence along the western edge of North America throughout the late Mesozoic and Cenozoic eras produced an orogen characterized as a mosaic of tectonostratigraphic terranes. The accretion and subsequent orogen-parallel displacement of these terranes can be explained by decoupling of the crustal terranes from the subducting lithospheric plate, accommodated by distributed plastic deformation throughout the lower crust.

Even at fast (greater than 100 mm/yr) convergence rates, distributed plastic deformation across the lower crust at conventional strain rates in the order of 10^{-13}/second can account for all of the relative motion between the converging plates, permitting complete crustal delamination. At slower convergence rates the ductile crust is thicker and possibly hotter, so that decoupling across the lower crust is increasingly favored.

Geologic evidence from the Coast Plutonic Complex supports this weak-lower-crust model. Exposures of deep crustal rocks are characterized by ubiquitous subhorizontal shear zone fabrics. At slightly shallower crustal levels displacements between relatively rigid blocks occurred along discrete steeply dipping shear zones.

T32C-5 1430h

The Dynamics of Compressional Orogenies: Beyond the Thin Sheet and Plane Strain Approximations...

Jean Braun (Research School of Earth Sciences, Australian National University, GPO Box 4, Canberra, ACT 2601, Australia)

Recent advances in numerical methods and computational means allow us now to study the dynamics of crustal deformation in three dimensions.

Predictions from a finite element model of an elasto-plastic crust subjected to finite shortening are used to better understand the physical processes at play during the formation and evolution (following finite deformation) of fold-and-thrust belts. We investigate quantitatively the effects on the large scale morphology of compressional orogens of the strength of crustal rocks, gravitational forces, the three-dimensional geometry of an assumed rigid basal decollement (made of a ramp and flats) and oblique convergence.

The results of a large number of numerical experiments (including computed topography, strain and stress distributions) are analyzed in terms of four dimensionless numbers: three geometrical factors ($\alpha=\Delta z/L$, ratio of the ramp height to deforming layer thickness, and φ and ϕ, the slope and tilt of the ramp) and a mechanical factor ($\mathbf{Ar}=\rho g L/T_0$, ratio of gravitational stresses to plastic strength).

The morphology of compressional orogens is shown to depend mostly on the thickness of the layer involved in the deformation and the geometry of the basal decollement.

T32C-6 1445h

Dynamic Models of Orogenesis and Post-Orogenic Collapse

Dennis L Harry, John S Oldow and Dale S Sawyer (Dept. of Geology and Geophysics, Rice University, P.O. Box 1892, Houston, TX 77251

A dynamic model of ocean-continent collision shows that orogen development is controlled by preexisting variations in the strength of the lithosphere which result from the presence of thick sediments at the continental margin and from variations in crustal thickness across the margin. A two-dimensional finite element method is used, in which the lithosphere behaves according to empirical brittle and ductile deformation relations. The continental crust is modeled with a 35 km thick dioritic basement overlain by a weaker 2.5 km thick sedimentary sequence. The sediments thicken to 15 km over the continental margin, and the basement thins to 7 km. The seaward edge of the sedimentary prism is bounded by 7 km thick gabbroic oceanic crust, which impinges on the continent at 5 mm/yr. In this simplified model, the oceanic lithosphere acts as a rigid indenter into the adjacent, relatively weak continental lithosphere. Strain initially focuses within the weak region encompassing the sedimentary prism, forming the orogen hinterland. Intense shortening, crustal thickening and uplift begins in this region immediately after the onset of collision. The amount of work required to continue crustal thickening within the hinterland increases as the orogen approaches its critical taper. By 50 m.y. after the onset of contraction it becomes energetically more favorable to deform the relatively thin crust in the foreland, and strain propagates toward the continental interior. Ductile slip within the lower crust beneath the orogen largely decouples strain in the crust from the mantle. The strong layer in the uppermost mantle may transmit strain as far as 500 km beyond the orogen into the continent interior. Thick crust and mantle roots develop near the foreland-hinterland transition, at the position of the landward edge of the sedimentary prism prior to contraction. The dense mantle root offsets the buoyancy of the crustal root, so that the greatest elevations do not lie above the thickest crust (they lie 150 km seaward). The mantle root is unstable, however, and begins to collapse via ductile flow in the lowermost lithosphere after about 100 m.y. This flow continues after the cessation of contraction, leading to complete elimination of the mantle root within 50 m.y. and rejuvenated uplift within the distal portions of the orogen.

T32C-7 1515h

N-S Extension on the Asian side of the Himalaya-Tibet Convergent System During Early Stage of Collision

Y. Pan, W.S.F. Kidd, Dept of Geology, SUNY Albany, NY 12222, T.M. Harrison, Dept of Earth and Space Sciences, UCLA, CA 90024, P. Copeland, Dept of Geology, Univ. of Houston, TX 77004

A substantial E-W striking ductile shear zone, ~1 Km wide and N-dipping, is found in the of the Quxu area within granitic rocks of the Gangdese plutonic belt, just north of the Indus-Zangbo suture. Mineral foliation dips to the north at 30-60° with prominent stretching lineation in the dip direction. Quartz c-axis measurements show a symmetric pattern in granitic rocks outside the shear zone and strongly asymmetric patterns within the shear zone. Kinematic indicators, including S-C fabric relation and oblique quartz shape preferred orientation, suggest that the main foliation has been formed by simple shear deformation with a top-to-north sense of shear. The lower grade phyllitic rocks in the upper part of this shear zone have also been sheared with clear evidence of normal faulting shear sense and it is observed in the field that the metamorphic grade drops from amphibolite facies to greenschist facies in a distance less than 100 m up the section. No convincing evidence exists for a rotated back thrust origin for this shear zone, although there are a few small (centimeter wide) E-W trending shear zones with thrusting shear sense in this general area. The crystallization age of granitic rocks south and north of this shear zone have been documented as 42 Ma and 50 Ma, respectively, and a hornblende $^{40}Ar/^{39}Ar$ age suggest that the rocks within this shear zone were crystallized at ~40 Ma. $^{40}Ar/^{39}Ar$ data from biotites and K-feldspars suggest that these sheared rocks have experienced slow cooling between 30 and 20 Ma at around ~10 °C/Ma, followed by faster cooling after 20 Ma, perhaps about 40 °C/Ma. This cooling history is essentially the same as that found north of the shear zone as documented by Copeland et al. (1987). A sharp increase of cooling rate for the area south of the shear zone also occurred around 20-18 Ma (our unpublished fission track data). We interpret this shear zone as a N-S extensional fault operating in the upper crust, likely at about 40 Ma (or possibly later but before 30 Ma), and its origin is probably similar to the younger large-scale E-W trending low-angle normal faults documented in the Higher Himalayas to the south of the suture zone.

T32C-8 1530h

Paleomagnetic Evidence for Clockwise Rotation in Eastern Qiangtang and Northern Indochina Terranes

Kainian Huang Department of Geology 1112 Turlington Hall University of Florida, Gainesville, FL 32611
N D Opdyke Department of Geology 1112 Turlington Hall University of Florida Gainesville, FL 32611

Paleomagnetic samples were collected from Cretaceous-Jurrasic redbed sequences from eastern Tibet, southern Yunnan, and southwestern Sichuan provinces of China. These sites are located northeast and east of the eastern syntaxis caused by the collision of India with Eurasia. Laboratory demagnetization and stability test indicate that characteristic directions resolved from these samples were acquired in the early history of the rocks. Compared with stable interior of Eurasia, the Cretaceous results reveal clockwise rotation of 39.7±13.0° to 57.7±17.0° for the sampling area of the eastern Qiangtang terrane, and 54.6±8.1° for southern Yunnan in northern Indochina terrane; latitudinal change is, however, insignificant since Cretaceous time. Southwestern Sichuan of western Yangtze block as well as the Dali area of western Yunnan, which is situated right on the Red River fault, shows no rotation. Jurassic results support these observations. Paleomagnetic data from the analogous region northwest and west of the western syntaxis seem to show a counterclockwise rotation. These data help to constrain differing hypotheses concerning the kinematics of the region resulting from the India/Asian collision.

T32C-9 1545h

The motion of South China as determined from the integration of strain rates

W.E. Holt and Ming Li, Department of Earth and Space Sciences, SUNY at Stony Brook, Stony Brook, NY 11794-2100
A.J. Haines, Department of Scientific and Industrial Research, Geology and Geophysics, Box 1320, Wellington, New Zealand

Here we investigate the complete kinematics of deforming Asia by fitting smoothed polynomials to observed values of strain rate. The complete kinematics of relative motion is defined by the spatial distribution of the rates of strain. That is, any suitable reference point or region can be chosen such that both relative velocities and rates of rotation can be determined everywhere within the zones where strain rates are matched by the smooth polynomial functions. Because the region of deforming Asia is large, we have determined the relative motions on a sphere. Strain rates are determined from summation of moment tensor elements of earthquakes in this century, and from estimates of Quaternary slip rates on some of the major faults. The motion of South China is defined by integration paths that cross the Tien Shan, the Altyn Tagh, Tibet, Gansu-Ningxia, W. Sichuan, and Yunnan. Results from the available strain rate data sets show that South China has a component of southward motion relative to northern Eurasia that is statistically significant (18±8 mm/yr). As well, South China appears to have a slight component of counterclockwise rotation relative to northern Eurasia (0.4 ± 0.25°/Ma). Other prominent features of the solution are rapid clockwise geodetic rotations in the Eastern Himalayan Syntaxis region and within the western parts of Yunnan and east Burma (around 1.5°-2°/Ma) relative to northern Eurasia and counterclockwise geodetic rotations in central and western Tibet relative to northern Eurasia (around 0.4-1.0°/Ma). These results are preliminary, since the data set has the obvious deficiency that it may not be representative of long-term strain rates. For this reason, we have investigated the sensitivity of the kinematics to assigned variations of the strain rate field. Ultimately we hope that estimates of Quaternary rates of slip on the major faults will provide sufficient constraints on the style and magnitude of long-term strain rate field in the various provinces.

T32C-10 1600h

Description of Brittle Deformation with Rigid Block Rotations: Classical vs Micropolar Continuum Models

R J Twiss, B J Souter (Dept. of Geology, Univ. of Calif. at Davis, Davis CA 95616-8605, USA; EMAIL: rjtwiss@ucdavis.edu)
J R Unruh (William Lettis & Associates, 1000 Broadway, Suite 612, Oakland CA 94607)

Classical continuum theory is inadequate to describe distributed brittle deformation with rigid block rotations. Micropolar continuum theory includes additional degrees of kinematic freedom that describe the effects of block rotations and lead to predictions of new patterns for slip directions and seismic **P** and **T** axes.

We assume that distributed brittle deformation occurs by sliding on shear planes that bound rigid blocks. The slip direction on a shear plane is the direction of maximum rate of shear, i.e. the direction of maximum rate of change of angle between two material lines **n** and **v**, which are unit vectors instantaneously normal to the shear plane and parallel to the slip direction, respectively.

Using classical continuum theory, any block must be bounded by a set of material planes in the continuum. The direction **v** of the maximum shear rate on any surface having a normal **n** is calculated by

$$v_m = \frac{1}{L}\left[d_{kj}\, n_k\, (\delta_{jm} - n_j\, n_m)\right]$$

where d_{km} is the symmetric part of the velociiy gradient tensor $v_{k,m}$ and δ_{jm} is the kronecker delta. Thus **v** is determinable from classical continuum theory, but *the block in this model must deform with the continuum, and it's spin cannot be different from that of the deforming continuum.*

If a block in the continuum is rigid, the rate at which **n** rotates is determined by $v_{k,m}$, which describes the continuum deformation, but the rate at which **v** rotates is determined by the spin of the block which is not uniquely determined by $v_{k,m}$. Thus we cannot use classical continuum theory to solve for the slip direction. Micropolar continuum theory represents the spin of the blocks by the microspin ω_{km} which describes extra degrees of rotational freedom for each point in the continuum. Thus the rotation rates of both **n** and **v** are determined, and the resulting slip direction is

$$v_m = \frac{1}{L}\{d_{kj}\, n_k\, (\delta_{jm} - n_j\, n_m) + (\omega_{km} - w_{km})\, n_k\}$$

where w_{km} is the antisymmetric part of $v_{k,m}$. The net spin (ω_{km} - w_{km}) represents the difference between the rotation rate of the rigid block and the average rotation rate of material lines in the continuum. It is an objective characteristic of the deformation, which means its magnitude is independent of the rigid motions of the reference frame. This quantity is not accounted for by classical continuum theory.

If fault slip during earthquakes is parallel to **v**, we can calculate theoretical patterns of seismic **P** and **T** axes. For a zero net spin, the pattern of slip directions on a uniform distribution of shear planes and the associated pattern of **P** and **T** axes have the same orthorhombic or

valley topography of a slow spreading center may reflect variations in recent magmatic heat input along a segment.

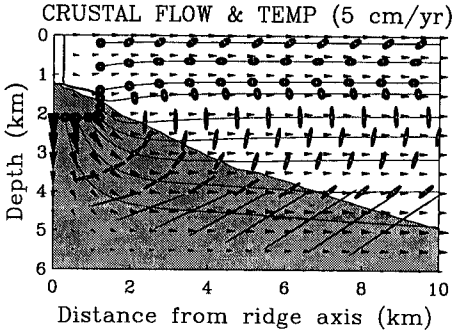

T32B-8 1545h INVITED

Tectonic Controls on Volcanic and Petrologic Segmentation of Ridges

W. Roger Buck (Lamont-Doherty Geological Observatory of Columbia University, Palisades NY 10964; 914-359-2900, ext. 592)

Diking at a spreading center tends to move an active normal fault away from the area of hottest thinnest lithosphere. When a normal fault is moved sufficiently far from a spreading center it should be replaced by another fault. Temporal variations in structures will result without temporal variations in the magma supply to the ridge. The tectonic and volcanic segmentation of ridges may partly be a result of different sections of ridges being in different stages of the evolution of the interaction of diking and faulting. A second idea discussed here is that some petrologic diversity may be a consequence of topographic segmentation of ridges. Several authors have noted that the density of magma is a function of the degree of fractional crystallization from a primary melt, and that generally the lowest density magmas are what make it to the seafloor. The difference in pressure head may allow denser than normal magmas from beneath shallow sections of ridge crests to migrate laterally and vertically to be extruded in deeper areas of a ridge crest. Thus, areas of considerable topographic relief would tend to be areas of more diverse magma types. Basalts rich in iron and titanium seem to fit this model in that they are often found in the deep areas of ridges with large topographic relief.

T32B-9 1600h

3-D Numerical Experiments on Buoyant Flow Beneath Segmented Spreading Centers

D.W. Sparks and E.M. Parmentier (Department of Geological Sciences, Brown University, Providence, RI 02912)
J. Phipps Morgan (Institute of Geophysics and Planetary Physics, University of California, San Diego, La Jolla, CA 92093-0225)

Oceanic spreading centers consist of offset ridge segments of various lengths exhibiting along-axis variations in topography, gravity, and the thickness and composition of crust. We are conducting 3-D numerical experiments on convection beneath a ridge-transform system driven by thermal and compositional buoyancy. The flow is composed of plate-driven flow in an asthenosphere overlying a more viscous half-space, and buoyant flow in an asthenosphere beneath a rigid lithosphere.

Buoyant flow takes the form of enhanced upwelling beneath the center of ridge segments and off-axis convective rolls oriented in the direction of spreading. These rolls, with the upwelling limb centered beneath the nearest ridge segment, are initiated by temperature gradients across fracture zones. It is important to understand the role of buoyant flow in evolution of plate boundary geometry. The strength of buoyant flow increases with decreasing spreading rate and mantle viscosity eventually dominating the pattern of deep upwelling, indicating that buoyant flow may determine the style of segmentation at slow spreading centers.

Buoyant flow creates large along-axis variations in the amount of melt produced and its composition. Assuming complete melt extraction and no along-axis migration, up to a threefold decrease in crustal thickness toward transforms is predicted explaining observed Bouguer gravity anomalies. Mantle density variations create a gravity anomaly which is smaller and more broadly distributed than that observed. At high viscosity the average depth and average degree of melting form a simple negative correlation, with the deepest and smallest degrees of melting beneath transforms. This may correspond to the local trend of Klein and Langmuir (JGR, 1989) observed at slow spreading centers. With decreasing viscosity distinctly different trends develop beneath the center of a ridge segment and near its transforms. The transform signature becomes more localized and off-axis upwelling contributes deep melt to the center of the segment.

T32B-10 1615h

Melt Compositions predicted from 3-D Flow Models: Local Trends and Transform Fault Effects

Yang Shen, David W. Sparks, E. M. Parmentier and Donald W. Forsyth (Department of Geological Sciences, Brown University, Providence, RI 02912)

At slow-spreading ridges, basalt compositions reflect a negative correlation between the average depth and average degree of melting, described as the "local trend" by Klein and Langmuir (JGR, 1989). This correlation, however, is not observed at fast-spreading ridges. A possible cause of this spreading-rate dependence is the three-dimensional nature of slow-spreading ridges, which have larger age-offsets and a stronger buoyant component of mantle upwelling. The "cold edge" of transform faults has been used to explain the variations in the degree of melting. We suggest, based on the published MORB compositions and our recent numerical experiments of 3-D mantle upwelling, that the transform fault effect is a self-consistent mechanism for the "local trend" in non-hotspot areas.

In our models, the temperature of deep mantle is fixed, causing the initial depth of melting to be relatively constant. At regions of reduced upwelling, melting stops at deeper levels, producing, on average, deeper and smaller degrees of melt. For passive flow models with temperature- and pressure- dependent viscosity, the deepest and smallest degrees of melting occur near large-age offsets. Buoyant flow enhances along-axis variations in upwelling velocity and the width of the melting region. As viscosity is decreased, the transform fault effect becomes more pronouced and localized. In addition, there is a transform-like signature beneath the center of segments, caused by a greater percentage of deep melt due to off-axis upwelling.

We estimate cumulative melt compositions along temperature profiles of our models. This is an improvement over adiabatic melting, because models including conductive cooling reaches the same degree of melting at shallower depth. Melting at shallower depths yields smaller values of FeO. With initial concentration of Na_2O and FeO of 0.27 and 7.55 wt% respectively, the trend for cumulative melt from different depths of a column has a slope similar to the observed "local trend". We speculate, however, that although the sampling of melts from different depths of a column may be helpful in shaping the "local trend", the variations in melting along the ridge axes are more important.

T32B-11 1630h

Mantle Flow Beneath Spreading Centers due to Mantle Depletion and Melt Retention Buoyancy

Kopal Jha and E.M. Parmentier (Department of Geological Sciences, Brown University, Providence, RI 02912)
J. Phipps Morgan (Institute of Geophysics and Planetary Physics, University of California, San Diego, La Jolla, CA 92093-0225)

Melt extraction changes the composition of residual mantle beneath spreading centers, principally reducing Fe/Mg, decreasing its density and creating mantle depletion buoyancy. Melt forming a connected network migrates rapidly. However, melt which is retained in the partially melting mantle has lower density than solid, creating melt retention buoyancy. This study examines mantle flow beneath a spreading center using numerical finite difference models following the basic formulation of an earlier study (Parmentier and Phipps Morgan, Nature, 1990). Mantle flow is approximated as flow in uniform viscosity halfspace due to 1) plate spreading 2) melt retention and mantle depletion buoyancy and 3) compaction resulting from melt extraction. Vertical melt migration by porous flow with a permeability that depends on melt fraction and grain size (Ahern and Turcotte, EPSL, 1979) controls the amount of melt present in partially melting, upwelling mantle. We adopted a relatively high melt viscosity (1 Pa-s) and small grain size (1 mm) to maximize the amount of melt present and therefore the importance of melt retention buoyancy.

We first considered 2D flow to examine flow structure and crustal thickness as a function of spreading rate and viscosity. These calculations were carried out in a region 600 km wide and 100 km deep with 129x51 grid points respectively. Melt retention and mantle depletion buoyancy both enhance and localize upwelling beneath the spreading axis relative to that for plate spreading flow alone. Mantle depletion buoyancy plays a fundamental role in controlling the flow structure by suppressing downward motion of diverging mantle beneath the spreading center, thus precluding the recycling of previously melted mantle through the region of melting. As with mantle depletion buoyancy alone (Sotin and Parmentier, GRL, 1989) crustal thickness becomes relatively independent of spreading rate when mantle viscosity is low enough for upwelling to be buoyantly dominated.

3D numerical experiments, started from a slightly perturbed 2D solution, examine the range of mantle viscosity and spreading rate for which 3D buoyant flow develops beneath a straight spreading axis. Flow was calculated in a region 300x600x100 km along axis, across axis, and depth with 33x65x25 grid points respectively. 3D flow develops for low spreading rate and low viscosity, conditions for which buoyancy driven upwelling is most important. For a given spreading rate, the 2D-3D transition occurs at higher viscosity than with depletion buoyancy alone. In a vertical plane along the spreading axis, melt retention buoyancy localizes upwelling more than mantle depletion buoyancy alone. The flow structure consists of regions of upwelling with adjoining regions where the vertical flow nearly vanishes: stable compositional stratification strongly inhibits vertical flow except in regions of melting. The along-axis localization of upwelling increases with decreasing viscosity.

T32C CC: 409A/B Wed 1330h

Dynamics and Kinematics of Plate Boundary Deformation

Presiding: W Holt, SUNY Stony Brook

T32C-1 1330h INVITED

MODELING OF THE DYNAMICS OF DISTRIBUTED SHEAR ALONG CONTINENTAL TRANSFORM BOUNDARIES

DAVID VERDONCK AND KEVIN P. FURLONG (Dept. of Geosciences, Penn State University, University Park, PA, 16802, davev@geosc.psu.edu, kevin@geosc.psu.edu)

Transform plate boundaries are normally thought of as simple, narrow regions of concentrated shear deformation. Although this may be the case along many oceanic transforms and perhaps for some continental transforms, deformation along continental transforms is often distributed over broad areas. The San Andreas system shows such distributed shear both in southern California (L.A., Borderlands) and in northern California (San Francisco Bay region). The location of deformation varies through the depth extent of the lithosphere leading to complex patterns of coupling between deformation in the upper crust and the deeper extent of the lithosphere.

In the San Francisco Bay region the total crustal displacement across the Pacific-North American plate boundary is distributed among several parallel fault strands. Geodetic data support a model where the deep motion is localized beneath the eastern portion of the fault zone. The difference in location of concentrated deformation between the crust and lower lithosphere requires a plate boundary structure which is more complicated than that of simple transform boundaries. Three-dimensional finite element models are used to investigate the effects of this complex fault geometry, lithospheric rheology, and variations in crust-mantle coupling on the deformational dynamics of this plate boundary. Preliminary results indicate that these variations in coupling between the upper crust and underlying mantle have a strong influence on the spatial pattern of deformation both at the surface and within the lithosphere. In regions with strong coupling the surface deformation is reflective of lower lithospheric processes. Weakly coupled regions behave almost independently of the deep deformation and show little to no internal crustal deformation. These complex patterns of shallow versus deeper deformation indicate the need for care in the inference of plate boundary processes from surface geodetic observations.

T32C-2 1345h

Flexural Modeling Along a Transform Plate Boundary: San Francisco Bay as a Result of Emplacement Terranes ?

Jordi Prims and Kevin P. Furlong (Dept. of Geosciences, Penn State University, University Park, PA 16802, jordi@ridge.geosc.psu.edu, kevin@geosc.psu.edu)

The San Francisco Bay region is part of a structural depression associated with the San Andreas transform plate boundary. This structural depression is not a 'pull-apart' associated with a dilational jog in the strike slip fault but rather has formed in association with a compressional jog in the San Andreas. Here we test whether the San Francisco Bay depression can be the result of flexural deformation associated with lithospheric loading caused by terrane movements along the plate boundary. The present bend in the San Andreas through the Santa Cruz Mountains, south and west of the San Francisco Bay, has led to both local crustal thickening in the Santa Cruz Mountains, and to the emplacement of crustal blocks (terranes) onto the Pacific plate in the region offshore of the San Francisco Peninsula. Both of these modifications to the regional crustal structure are investigated in terms of their possible role in creating the Bay depression. Subsidence of the San Francisco Bay region occurred since the Pleistocene and Holocene and continues today (although presently at a low rate). Although the Santa Cruz mountain segment of the San Andreas is older than this period of subsidence, the spatial correlations between regions of crustal thickening and the Bay argue for a possible link. For this reason we have explored the lithospheric flexural response to the emplacement of Salinia terrane in offshore Central California and mountain building. The San Francisco Bay Depression and Santa Cruz Mountains may be the result of the complex fault geometry and specific crust-mantle kinematics of the area, accommodating the lithospheric deflection generated by modifications to crustal structure on the Pacific Plate.

T32C-3 1400h

Constraints on the Mechanical Behavior of Forearcs from Slip Vector Azimuths and Oblique Plate Convergence

Robert McCaffrey (Department of Earth & Environmental Sciences, Rensselaer Polytechnic Institute, Troy, NY 12180; robmcc@harold.geo.rpi.edu)

Gradients in the obliquity of convergence along a subduction zone result in a trench-parallel horizontal shear force being applied to the forearc of the upper plate. Deviations of earthquake slip vectors from the plate convergence direction tell us about the trench-parallel deformation rates within the forearcs. By observing the slip vectors as a function of obliquity we can constrain the behavior of forearcs and make inferences about their rheology. Calling ψ the angle the earthquake slip vector azimuth makes with the trench-normal azimuth and γ the obliquity (plate vector minus trench-normal), the theoretical relationship between them is:

$\psi(\gamma) = (1-\alpha)\tan\gamma + \alpha\tan\gamma_c \quad \gamma > \gamma_c$

$\psi(\gamma) = \gamma \quad \gamma \le \gamma_c$

which incorporates elastic, elastic-perfectly plastic, elastic-plastic, and viscous behavior of the forearcs depending on the values of the two parameters α and γ_c. γ_c represents the obliquity at which the forearc's plastic yield stress is reached.

T

MONTREAL
May 12–16, 1992

1992 SPRING MEETING

American Geophysical Union
Canadian Geophysical Union
Mineralogical Society of America

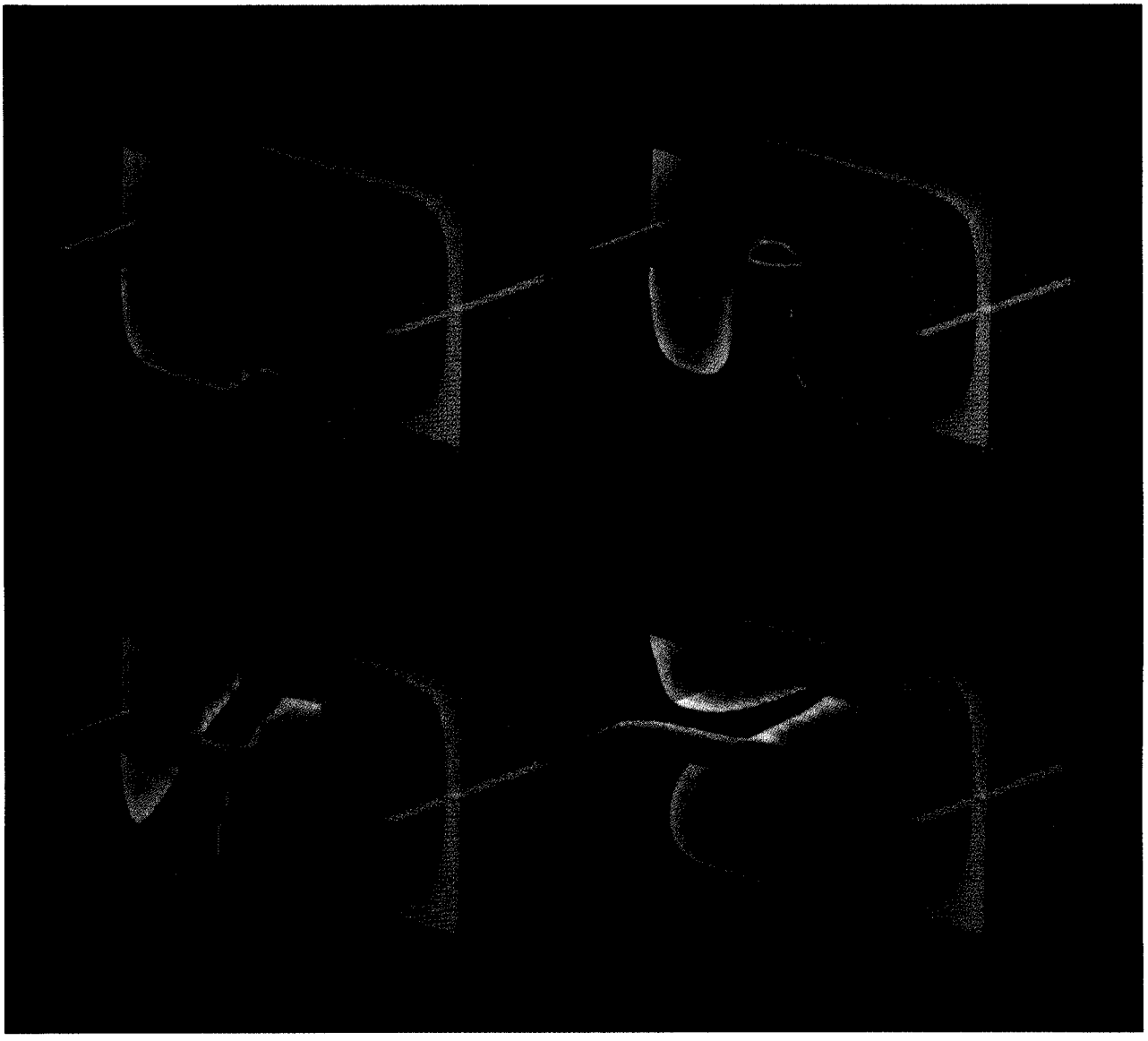

Published as a supplement to *Eos*, April 7, 1992

EOS, TRANSACTIONS, AMERICAN GEOPHYSICAL UNION
1992 SPRING MEETING
VOL. 73, NO. 14, APRIL 7, 1992 / SUPPLEMENT